SAND2018-13133J

Title: A decade of remotely sensed observations highlight complex processes linked to coastal permafrost bluff erosion in the Arctic

Authors: Benjamin M. Jones[1], Louise M. Farquharson[2], Carson A. Baughman[3], Richard M. Buzard[4], Christopher D. Arp[1], Guido Grosse[5], Diana L. Bull[6], Frank Günther[5], Ingmar Nitze[5], Frank Urban[7], Jeremy L. Kasper[8], Jennifer M. Frederick[6], Matthew Thomas[9], Craig Jones[10], Alejandro Mota[11], Scott Dallimore[12], Craig Tweedie[13], Christopher Maio[4], Daniel H. Mann[4], Bruce Richmond[14], Ann Gibbs[14], Ming Xiao[15], Torsten Sachs[16], Go Iwahana[17], Mikhail Kanevskiy[8], and Vladimir E. Romanovsky[2]

[1] Water and Environmental Research Center, University of Alaska Fairbanks, Fairbanks, AK USA
[2] Geophysical Institute, University of Alaska Fairbanks, Fairbanks, AK
[3] Alaska Science Center, U.S. Geological Survey, Anchorage, AK, USA
[4] Geoscience Department, University of Alaska Fairbanks, Fairbanks, AK, USA
[5] Alfred Wegener Institute Helmholtz Centre for Polar and Marine Research, Potsdam, Germany
[6] Sandia National Laboratories, Albuquerque, NM, USA
[7] Geosciences and Environmental Change Science Center, U.S. Geological Survey, Denver, CO, USA
[8] Institute of Northern Engineering, University of Alaska Fairbanks, Fairbanks AK, USA
[9] Geologic Hazards Science Center, U.S. Geological Survey, Golden, CO, USA
[10] Integral Consulting, Santa Cruz, CA, USA
[11] Sandia National Laboratories, Livermore, CA, USA
[12] Geological Survey of Canada, British Columbia, CA
[13] University of Texas El Paso, El Paso, TX, USA
[14] Pacific Coastal and Marine Science Center, U.S. Geological Survey, Santa Cruz, CA, USA
[15] Department of Civil & Environmental Engineering, The Pennsylvania State University, University Park, PA, USA
[16] GFZ German Research Centre for Geosciences, Potsdam, Germany
[17] International Arctic Research Center, University of Alaska Fairbanks, Fairbanks, AK, USA

Abstract

Eroding permafrost coasts are indicators and integrators of changes in the Arctic System as they are susceptible to the combined effects of declining sea ice extent, increases in open water duration, more frequent and impactful storms, sea-level rise, and warming permafrost. However, few observation sites in the Arctic have yet to link decadal-scale erosion rates with changing environmental conditions due to temporal data gaps. This study increases the temporal fidelity of coastal permafrost bluff observations using near-annual high spatial resolution (<1 m) satellite imagery acquired between 2008 and 2017 for a 9-km segment of coastline at Drew Point, Beaufort Sea coast, Alaska. Our results show that mean annual erosion for the 2007 to 2016 decade was 17.2 m yr^{-1}, which is 2.5 times faster than historic rates, indicating that bluff erosion at this site is likely responding to changes in the Arctic System. In spite of a sustained increase in decadal-scale mean annual erosion rates, mean open water season erosion varied from 6.7 m yr^{-1} in 2010 to more than 22.0 m yr^{-1} in 2007, 2012, and 2016. This variability provided a range of coastal responses through which we explored the different roles of potential environmental drivers. The lack of significant correlations between mean open water season erosion and the environmental variables compiled in this study indicates that we may not be adequately capturing the environmental forcing factors, that the system is conditioned by long-term transient effects or extreme weather events rather than annual variability, or that other not yet considered factors may be responsible for the increased erosion occurring at Drew Point. Our results highlight an increase in erosion at Drew Point in the 21st century as well as the complexities associated with unraveling the factors responsible for changing coastal permafrost bluffs in the Arctic.

Introduction

Permafrost influences 30 to 34 % of Earth's coastlines (Walker 2005, Lantuit et al., 2012). Ongoing and anticipated changes in the Arctic System such as reductions in sea ice extent (Perovich et al., 2017), rising air (Overland et al., 2017) and sea surface temperatures (Steele and Dickinson, 2016), relative sea-level rise (Richter-Menge et al., 2011), warming permafrost (Romanovsky et al., 2010; Smith et al., 2010), and increased storminess (Simmonds et al., 2012) involving more frequent storm surges (Vermaire et al., 2013) may all interact to amplify arctic coastal dynamics (AMAP, 2017). Changes in the Arctic System will likely increase the vulnerability of these coasts to erosion and alter coastal morphologies, ecosystems, carbon export to oceans, infrastructure, and human subsistence lifestyles (Arp et al. 2010; Radosavljevic et al., 2016; Fritz et al., 2017; Obu et al., 2017; Couture et al., 2018; Farquharson et al., 2018).

Despite the prevalence of permafrost coasts in the circumpolar north and their apparent vulnerability to change, there remains a paucity of information regarding their recent dynamics and how this varies spatiotemporally. Lantuit et al. (2013) identified only 15 coastal change detection studies conducted between 2008 and 2012 accounting for less than 1 % of the Arctic permafrost coastline. Further, since most coastal change detection studies report rates averaged over years to decades, it is difficult to determine the relations between changes in environmental forcing and the response of the coast. For example, Lantuit et al. (2011) assessed the change in mean annual erosion rates for the Bykovsky Peninsula in Siberia and found no connection with the storm climatology for the region over the 55 year study period. In a different region, Overeem et al. (2011) indicated that the duration of open water conditions could be a good first order predictor of coastal erosion based on similar increases in open water duration and erosion rates for 1979-2002 and 2002-2007 for Drew Point, Alaska.

Better understanding short-term coastal dynamics in the Arctic is important because erosion of permafrost coastal bluffs impacts infrastructure, subsistence activities, wildlife habitat, and the permafrost carbon feedback. Hotspots of coastal erosion may be ideal locations to explore the direct impact of specific environmental forcing factors on Arctic coastal dynamics because higher rates can be detected more accurately with remote sensing data. In this study, we combined the use of high-spatial resolution (sub-meter) satellite imagery derived from optical sensors (Quickbird, IKONOS, GEOEYE, Worldview-1 and -2) to document a decade of annual open water season erosion along a 9-km segment of the Alaska Beaufort Sea Coast (ABSC) located near Drew Point (Figure 1). Drew Point provides a potential indicator site for anticipating changes in ice-rich permafrost coastal bluffs because this coastline is located in a zone of rapidly changing sea-ice cover. Our decade-long time series was then placed in the context of historic remote sensing observations for the site between 1955 and 2007 (Jones et al., 2009a). Our study attempts to directly link the sweeping changes occurring in the Arctic System over the last decade with coastal permafrost bluff erosion at an erosional hotspot on the ABSC. The unprecedented time series of eroding permafrost coastal bluffs facilitated correlation testing of annual erosion with open ocean water duration, sea surface temperature, storm number, cumulative storm strength, thawing degree days, and near-surface permafrost temperatures.

Study Area

Alaska Beaufort Sea Coastal Setting and Drew Point

The ABSC is composed of a low-lying (maximum elevation of ~10 m) tundra plain that extends ~1,950 km from the Canadian Border to Utqiaġvik (formerly Barrow), Alaska, USA. Spatial and temporal rates of coastal change along the ABSC are known to be highly variable (Jorgenson and Brown, 2005; Lantuit et al., 2012; Gibbs and Richmond, 2015, 2017), due to variability in ground-

99 ice content (and wedge-ice content in particular) as well as variation in erosional processes,
100 geomorphology, lithology, coastal orientation, near shore bathymetry, and the presence of barrier
101 islands (Jorgenson and Brown, 2005). Jorgenson and Brown (2005) and Gibbs and Richmond
102 (2015) reported that the long-term average erosion rate along the ABSC between the late-1940s
103 and early-2000s was ~2 m yr^{-1}. However, some particular sites eroded as much as 16 to 20 m yr^{-1}.
104 Ping et al. (2011) assessed 48, 1-km segments distributed across the ABSC and found that mean
105 annual erosion between 1950 and 1980 was 0.6 m yr^{-1}, but increased to 1.2 m yr^{-1} between 1980
106 and 2000. Mars and Houseknecht (2007) compared land loss due to erosion by differencing
107 Landsat satellite imagery with legacy topographic map sheets and also found a doubling in the rate
108 of erosion between 1985 and 2005 relative to 1955 and 1985. Jones et al. (2009a) used more
109 precise techniques based on aerial photography for the exposed and north-facing, 60-km segment
110 of the ABSC between Cape Halkett and Drew Point and found that the erosion rate increased from
111 6.7 m yr^{-1} (1955 to 1979), to 9.7 m yr^{-1} (1979 to 2002), to 13.6 m yr^{-1} (2002 to 2007). Barnhart et
112 al. (2014) reported that the mean erosion rate over a 7-km stretch of coast at Drew Point was 15 m
113 yr^{-1} (2008–2011) and 19 m yr^{-1} (2011–2012).

114 We focus on a 9-km stretch of the Drew Point coastline located in the western region of
115 the ABSC about 100 km east of Utqiaġvik and 200 km west of Prudhoe Bay (Figure 1). The
116 dominant erosional process at Drew Point consists of thermo-abrasion (Jones et al., 2009a),
117 although thermo-denudation also occurs here (Wobus et al., 2011) (Figure 2). Bluff height ranges
118 from 1.6 m to 7.1 m, with a mean of 4.4 m above the mean water level during LiDAR data
119 acquisition on 6-Aug-2011. The near surface sediments consist mainly of ice-rich Holocene-aged
120 lacustrine silts with local peat accumulations and contain large ice wedges. Sediments underlying
121 lacustrine silts consist of transgressed marine late Quaternary silts and clays with sandy horizons

near the base of the eroding bluffs. Estimates of total volumetric ground-ice content for permafrost along these bluffs approaches 80-90 %, (Kanevskiy et al., 2013), with segregated and pore ice volumes accounting for 50 to 80 %, and wedge ice contributing nearly 30% in some locations (Wobus et al., 2011). The fine grained composition of the bluffs, means that eroded sediment is easily transported away and does not accumulate and protect the base of the bluffs as is common elsewhere. Estimates of ice-wedge polygon dimensions, range from 6 to 25 m across with a mean size of ~15 m (Wobus et al., 2011; Kanevskiy et al., 2013). Ice wedges are approximately 1 to 4 m wide near the surface and typically penetrate 3 – 5 m down from the surface. The Drew Point area is underlain by continuous permafrost with mean annual ground surface temperatures of about -9 °C (Smith et al., 2010). Permafrost at a depth of 20 m at coastal sites along the ABSC has warmed by 0.6 °C to 2.2 °C between 1989 and 2008 (Smith et al., 2010).

Offshore, water depths are shallow, the open water season is short, and the tidal range is on average only 15 cm. Nearshore water depth is less than 2 m within a distance of 0.5 km from the shoreline and increases to 3 m at a distance of 2.0 km from the coast. The nearshore open water duration at Drew Point has more than doubled between 1979 and 2009, increasing from ~45 days to ~90 days, with a higher proportion of the increase in open water duration occurring in the fall (~0.9 days yr^{-1}) relative to the early summer (~0.7 days yr^{-1}) (Overeem et al., 2011). However, this area is prone to highly variable open water seasons and is influenced by sea-ice transport and break-up patterns from both the east and the west (Barnhart et al., 2016). Between 2007 and 2012, the Beaufort Sea experienced the lowest September sea ice extents yet observed since the late 1970s (Ballinger and Rogers, 2013) and has continued to exhibit similar patterns through 2017 (Perovich et al., 2017). This increase in open water days has been accompanied by a warming trend in sea surface temperature (SST) in the Beaufort Sea (Steele and Dickinson, 2016). Air

145 temperature has continued to increase in this region since 2000 as measured near Utqiaġvik, AK
146 (Wendler et al., 2012).

147 Rapid shoreline retreat rates observed along the ABSC may partially be explained by
148 erosional processes uniquely associated with ice-rich permafrost coastal bluffs (Are, 1988;
149 Dallimore et al., 1996). Lantuit et al. (2008a) demonstrated a weak but statistically significant
150 relation between ground-ice content and mean retreat rate, with higher mean annual retreat rates
151 typically corresponding to coastlines with higher ground-ice content. Block failure following
152 undercutting caused by thermo-abrasion and thaw slump activity (thermo-denudation) are
153 common modifiers of Arctic coastal morphology and tend to be dominant erosional processes
154 along ice-rich permafrost bluffs (Are, 1988; Walker, 1988; Günther et al., 2012). Melting of
155 ground ice is an important consideration as it can substantially reduce the volume of sediment
156 input and cause thaw settlement in the nearshore, deepening the nearshore profile. Interestingly,
157 observations made along this coast in 1901 (Schrader, 1904) indicate that collapsed blocks could
158 persist for 4 to 5 years (Leffingwell, 1919). Such observations highlighting that both the formation
159 of erosional-niches followed by block collapse have been modifying this coast for at least the last
160 century and that the combined impacts of climatic-oceanographic-geomorphologic conditional
161 states have changed dramatically since the early 1900s.

162 # Data and Methods

163 ## Remote Sensing Observations and Geospatial Analysis

164 The primary objective of this study is to map coastal permafrost bluff changes and compare annual
165 retreat rates with annual open water season duration and other factors to better understand the
166 potential mechanisms responsible for the reported increase in erosion observed at Drew Point since
167 the early 2000s (Jones et al., 2009a; Overeem et al., 2011; Barnhart et al., 2016). We acquired ten

168 suitable high spatial resolution satellite images from five different satellites: Quickbird, IKONOS,
169 GEOEYE-1, and Worldview-1 and -2 (Figure 3) for a 9-km segment of eroding permafrost bluffs
170 located at Drew Point, Alaska, USA between 2008 and 2017. We only used the high-resolution
171 panchromatic band provided by each of these satellites, with spatial resolutions between 0.5 and
172 1.0 m. The number of shoreline observations acquired in this study is 10, a significant increase
173 from the previously available high spatial resolution observations, which was 4, for this site since
174 the 1950s.

175 Airborne LiDAR data was acquired on 6 August 2011 for our study area, which provided
176 a common base layer for georectifying all of the imagery. Initially, optical images were
177 automatically orthorectified using the RPC information embedded in the image file and the LiDAR
178 DTM (1 m postings), but the results showed variability in the position of ice-wedge intersections
179 on the order of 2 to 5 m. To improve image rectification, we selected 20 ground control points per
180 image using the LiDAR DTM as the base map. A second order polynomial transformation was
181 applied resulting in the images being georectified to UTM NAD83 Zone 5N, with spatial
182 resolutions ranging from 0.5 m to 1.0 m. The mean RMS associated with the georegistration
183 process ranged from 0.44 m to 0.85 m (SOM Table 1), with a maximum individual registration
184 point RMS error always less than 1.5 m. Visual comparison of each optical image strip for our
185 study area showed excellent spatial agreement and suitability for further analysis in spite of
186 differing image acquisition conditions. Difficultlies in the use of automated approaches for
187 delineating blufflines in high-spatial resolution optical imagery (as recently noted by Lantuit et al.
188 (2011) and Günther et al. (2013, 2015)) required manual delineation of the coastal permafrost bluff
189 line. The bluff line was manually digitized in each image independent of one another at a scale of

190 1:1,000. We also included the bluff line position from 2007 aerial photography as reported in
191 Jones et al. (2009a) to expand annual coverage and have a complete decade of annual observations.
192 Bluff position measurements were made at 10 m increments along the study coast using
193 the Digital Shoreline Analysis System (DSAS v. 4) (Thieler et al., 2017). This tool measures the
194 change in distance between two vector lines relative to a baseline and is widely used to measure
195 coastal changes in the Arctic (Jones et al., 2008, 2009a, 2009b; Gibbs and Richmond, 2015, 2017;
196 Farquharson et al., 2018). The baseline in our study was created by taking a buffer of the 2007
197 shoreline and isolating the offshore line vector. Transects were cast every 10 m along this baseline
198 using a 200 m smoothing algorithm to account for subtle undulations in the coastline and to ensure
199 perpendicular transects. This resulted in 888 transects along the ~9 km baseline. Since two small
200 segments of this coast represent areas with small streams flowing into the ocean without exposed
201 coastal bluffs, these were removed from further analysis. The end result provided a measure of
202 bluff line erosion along the study coast at 876 measurement points annually for the past decade.
203 While it is difficult to accurately assess errors in erosion rate measurements associated with
204 this type of analysis (Lantuit et al., 2011), we adopted techniques used in previous coastal change
205 detection studies (Hapke, 2005; Lantuit and Pollard, 2008b; Jones et al., 2009a; Gorkhovich and
206 Leiserowiz, 2011; Gibbs and Richmond, 2017). These are based on the identification of factors
207 that contribute to the error associated with feature delineation in the images under comparison
208 (SOM Table 1). Potential sources of error include the spatial resolution of the imagery, the RMS
209 error associated with image registration, and the ability to accurately map the bluffline in the same
210 optical image, as a proxy for producers uncertainty as averaged from the digitization of the same
211 image three times (SOM Table 1).
212

213 **Nearshore Marine Observations**

214 We extracted daily and bi-daily sea-ice concentrations at Drew Point between 1979 and 2016 using
215 Nimbus-7 SMMR and DMSP SSM/I-SSMIS Passive Microwave Data from the National Snow
216 and Ice Data Center (NSIDC) to define annual open water periods (Overeem et al. 2011). Using
217 three, 25-km^2 nearshore pixels, sea-ice concentrations < 15% were flagged as open water. The
218 open water duration was defined as the average of these three pixels exhibiting less than 15 % sea
219 ice concentration in a given year. The first, last, and total number of open-water days per year for
220 each sampled pixel were compiled for the study period (Figure 4). Sea surface temperature data
221 were derived from the NOAA Optimum Interpolation (OI) Sea Surface Temperature (SST) V2
222 dataset (Reynolds et al., 2002) for the three grid cells located between 71 °N to 72 °N and 154 °W
223 to 152 °W. Weekly sea surface temperature data were averaged for the various open water periods
224 determined with the NSIDC open water duration dataset. Locally, a time lapse camera was also
225 installed on a pipe anchored into the subsea permafrost in August 2016 and provided hourly images
226 for determining the wind speed and direction necessary for conducting geomorphic work which
227 was used to determine storm conditions of interest (Figure 5).

228 **Atmospheric and Terrestrial Observations**

229 Onshore, we collected hourly data for wind speed and direction and air and ground temperatures
230 using the U.S. Geological Survey meteorological station which has operated at Drew Point since
231 1998 (Urban and Clow, 2016). We compiled hourly air temperature data from June to October to
232 characterize the summer season, wind speed/direction data for the open water period for each
233 respective year, and near-surface summer/fall (June to October) permafrost temperature data from
234 2007 to 2016. The hourly air temperature data have been summed to daily means and used to
235 calculate the number of thawing degree days (based on 0 °C) for each period. The wind data and

the time lapse camera (Figure 5) were used to identify wind events or storms capable of forming erosional niches at the bluff base and/or collapsed block degradation (Figure 5). The time lapse images showed that the geomorphologically significant winds were generally those with wind speeds greater than 5 m/s from directions of 240° to 360° and 0° to 90°. Thus, we modified the methods of Atkinson (2005) to represent winds exceeding 5 m/s from the directions mentioned above for a period of at least 12 hours with no lulls > 6 consecutive hours. Each wind or storm event was further summarized according to a storm-power metric (Atkinson, 2005) taken as the square of a storm's average wind velocity relative to its duration. The various open water duration assessments were used to summarize storms or winds indicative of conducting geomorphic work in a given open water period. Permafrost temperature data were aggregated to summer/fall (June to November) seasonal means.

Results and Discussions

Increase in Erosion Rates at Drew Point during the 21st Century

Early 21st century, mean annual erosion has increased at Drew Point, ABSC when compared to the latter half of the 20th century (Figure 6a). The increase in erosion reported in Jones et al. (2009a) for the period 2002 to 2007 (16.3 m yr^{-1}) relative to the 1955 to 1979 (7.0 m yr^{-1}) and 1979 to 2002 (9.4 m yr^{-1}) time periods has been sustained between 2007 and 2016 (17.2 m yr^{-1}). This indicates that changes observed at this particular site are likely linked to ongoing shifts in the atmospheric, terrestrial, and/or marine conditions increasingly typical of the warming 21st century Arctic and not the result of enhanced erosion associated with a few catastrophic events where 25-40 m of erosion in a single year can have a big impact on the decadal-scale average (Are 1988, Lantuit et al., 2012). In spite of a sustained increase in erosion of 17.2 m yr^{-1} at Drew Point, year to year variability in open water season erosion was as high as 15.9 m. The range in mean annual

erosion of 6.7 m in 2010 to more than 22.0 m in 2007, 2012, and 2016 (Figure 6b) provided the basis for standardizing nearly annual observations of coastal bluff change using the number of open water days between image acquisitions to explore various environmental drivers.

Evaluating Erosion Patterns based on Open Water Duration

Erosion rates are typically reported on annual to decadal time-scales in the Arctic but focusing on the open water period when erosion is occurring may better resolve the processes driving coastal permafrost bluff retreat (Overeem et al., 2011). Our nearly annual time series of high resolution satellite images allowed us to constrain open water season erosion between 2007 and 2016. In Table 1, we report an erosion year which refers to the roughly annual period of image observations available for our study coast. Between 2007 and 2016, the average open water duration (OWD) was 91 days, but it ranged from 71 days (2014) to 107 days (2008 and 2016). In 2010, open water duration erosion was 0.08 m day^{-1} and more than 0.20 m day^{-1} in 2007, 2012, 2014, 2015, and 2016 (Table 1). However, the difference in open water duration season did not correspond to periods of the lowest and highest observed coastal bluff losses. In 2008, 2009, and 2011-2014 the ability to bracket the open water period in a given year was not possible. However, OWD as derived from satellite remote sensing data constitutes our erosion year and thus we have considered the timing of image acquisition relative to measured erosion and accounted for this when summarizing erosional losses and open water days. Thus, when assessing erosion on a near-annual basis, the hypothesis that OWD is a good first order predictor of coastal erosion at Drew Point does not hold up.

Evaluating Erosion Patterns based on Multiple Forcing Factors

Factors contributing to patterns of coastal bluff retreat include open water season, sea surface temperature, summer air temperature, and permafrost temperature, yet few studies have explored their correlation with rates of erosion (Figure 7). Barnhart et al. (2014) indicated that the combination of OWD and the number of storms during this period were important factors controlling erosion at Drew Point. On average, there were ~11 storms per year between 2007 and 2016. In the 2010 erosion year, the year with the lowest measured bluff retreat of 6.7 m, the fewest storms occurred (n=8) and in the 2012 erosion year, the year with the highest measured bluff retreat 22.6 m, the most storms occurred (n=17). While the assertion that the combination of the number of storms during an open water period holds true at Drew Point on the extreme end of observations, we find that the correlation between the two variables over the study period yields a low R^2 (0.21) (Figure 7) and an attempt to correlate variability in cumulative storm strength in a given erosion year yielded even lower relations (R^2 = 0.09). We also correlated mean erosion year variables indicative of sea surface temperature, summer air temperature, and permafrost temperature, and all were weak and not statistically significant (Figure 7). Multiple linear regression, forward stepwise regression, and best subsets regression of our erosion year open water season time series at Drew Point did not reveal any statistically significant relations either.

Permafrost Coasts as an Indicator of Arctic System Change

Do the dynamics of permafrost coastlines serve as critical indicators of changes in the Arctic System? Answering this question in a definitive way is difficult because few studies describe coastal erosion rates on an annual basis or during the most recent and rapid period of environmental changes. Based on decadal time-scales, observations at Drew Point, two additional examples from the ABSC, one from the Canadian BSC, and one from the Laptev Sea region in Siberia indicate an

303 increase in permafrost coastal bluff erosion since the early 2000s. Tweedie et al. (2012)
304 documented recent annual erosion trends of 1 to 4 m yr^{-1} between 2003 and 2011, which is 2 to 4
305 times higher than historic rates reported for their ~11-km study coast in Elson Lagoon in the
306 western ABSC (Brown et al., 2003). Along the eastern ABSC, Gibbs et al. (2018) report that
307 erosion along permafrost coastal bluffs at Barter Island increased from 1.6 m yr^{-1} (1979 to 2003)
308 to 5.5 m yr^{-1} (2003-2017), a 3.4 fold increase. Irrgang et al. (2018) report that decadal-scale erosion
309 measured along a 210 km reach of the Yukon Territory mainland Canadian BSC increased from
310 0. 5 m yr^{-1} (1970 to 1990) to 1.3 m yr^{-1} (1990 to 2011), a 2.6 fold increase. Observations from
311 coastlines backed by syngenetic permafrost in the Laptev Sea region in Siberia also indicate
312 erosion rates 1.5 to 3 times higher in the early 2000s relative to the period between 1950 and 2000
313 (Günther et al., 2013, 2015). Thus, despite a poor correlation between any one environmental
314 factor and rates of coastal erosion, accumulating evidence indicates multiple Arctic coastal sites
315 have experienced increased erosion of permafrost coastal bluffs during the 21st Century.
316 ***What factors appear to be responsible for an increase in permafrost coastal erosion?*** The
317 detailed spatiotemporal observations between 2007 and 2016 presented in this study provide a
318 range of coastal bluff loss magnitudes and variability in environmental conditions to attempt to
319 partition out the factors most responsible for the increase in erosion since the early 2000s.
320 However, there was no clear overarching factor or combination of factors that we compiled that
321 could explain the high spatiotemporal erosion observations made possible at Drew Point with the
322 satellite imagery. Annual observations from the Elson Lagoon study site on the western ABSC
323 indicate that differences in sampling periods with high and low wave-driven wind activity
324 influence bluff line erosion magnitude but correlations were inconclusive (Tweedie, et al., 2016).
325 At Muostakh Island in the Laptev Sea, the two most important controls on annual erosion are OWD

and summer air temperatures, with variation in TDD sums explaining the most variation (R^2=0.95) (Günther et al., 2015). However, observations over a period of 3 years or more highlight the importance of the coupled erosion of thermo-abrasion and thermo-denudation operating together in maintaining year-to-year trends in erosion (Günther et al., 2015), the former of which we cannot directly measure with the satellite imagery used in this study. What these comparisons may illustrate is that there is no "one size fits all" explanation for how Arctic coastlines will respond to changes in the Arctic System, a finding which highlights the need for regional based studies in the future.

How do various environmental forcing factors interact with one another to drive coastal permafrost bluff erosion? The seasonality of coastline retreat and interannual variations of environmental factors suggest that increases in erosion are driven by lengthened periods of thermo-denudation and thermo-abrasion activity (Günther et al., 2015). Interestingly, at Drew Point, multivariate analyses of the environmental data do not show significant correlations with our open water season erosion time series and thus failed to provide supporting evidence for this hypothesis. However, differences in the geological and geomorphological settings between the ABSC and the East Siberian coastline have to be considered in this regard, as in the latter region subaerial ground ice ablation at >20 m high bluffs may be more sensitive to air temperature increases compared to the low elevation thermo-abrasion dominated ABSC. The lack of significant correlations between mean annual erosion and the suite of environmental variables compiled in this study means we are likely not accurately capturing all of the environmental forcing factors at adequate resolutions or accuracies, that the system is conditioned by long-term transient effects or extreme weather events rather than annual variability, or that other not yet considered factors may be responsible for the increased erosion occurring at Drew Point.

One such factor might be related to the enhanced development of a cryopeg at Drew Point during the past several decades of permafrost warming in the region. During a drilling campaign conducted in April 2018, we encountered a cryopeg at Drew Point that ranged in elevation from 0.3 m asl to > 2.3 m bsl. Ground temperature at this depth was ~ -8 °C yet the material was primarily unfrozen. It is conceivable that the 3-4 °C permafrost warming in the region over the past several decades has increased the erodibility of the saline permafrost deposits located at this critical elevation where thermo-erosional niches actively develop during periods of elevated ocean water levels. Additionally, since the block failure erosion mode is of erratic nature and nonlinear, interactions and dependencies of erosion rates to environmental forcing factors might have become blurred due to onshore resistance forces resulting from a predetermined ice wedge polygon system. While Overeem et al. (2011) suggested that erosion occurring at Drew Point is non-fetch limited, including fetch in our analysis might also help to boost our ability to predict erosion at the site. In the open water season of 2012, for example, Thomas and Rogers (2014) highlight that waves in the Beaufort Sea developed beyond pure wind-driven seas and evolved swells, which can travel further and have long-distance impacts in an ice free sea.

Better Constraining Arctic Coastal Changes

Our study underscores the challenge in using remotely-sensed snapshots of landscape change to confidently identify the processes driving the observed increase in coastal permafrost bluff erosion rates along the ABSC. While our datasets facilitated a continuous suite of observed erosion over a decade for Drew Point, complex oceanographic and geomorphic feedbacks limit the ability of our approach to discern the impact of various environmental forcing factors. For example, empirically-based modeling approaches that have been employed in the Drew Point area have experienced a similar kind of limitation regarding process-based understanding. Our

work, taken within the context of contributions from the rapidly-emerging Arctic coastal research community, encourages the pairing of carefully-designed field monitoring and multi-physics (i.e., oceanographic, thermal, and mechanical) model development. Taken together, this kind of "measure and model" approach may further elucidate the sensitivities of Drew Point (and other indicator sites in the Arctic) to uncertain environmental futures.

Conclusions

Mean annual decadal-scale erosion rates during the early 21st century at Drew Point, Alaska are 2.5 times faster than historic rates measured between 1955 and 1979. While the present work provides a reliable observational dataset of erosion at Drew point, the nonlinear interaction between the environmental forcing factors responsible for erosion will require longer term measurements. The lack of significant correlations between mean annual erosion and the suite of environmental variables compiled in this study indicates that a longer term dataset is necessary before developing conclusions as to the interaction of forcing factors responsible for increased erosion occurring at Drew Point. Local occurrence of saline permafrost horizons that transform to an unfrozen state under generally warming conditions but still sub-zero temperatures compared to surrounding ice-rich permafrost, may possibly serve as one of those. Our analyses point towards the potential benefit of higher temporal resolution coastal observations and/or improved spatial resolution environmental datasets to better isolate and partition factors controlling erosion responses to environmental change. Our results highlight a sustained increase in erosion at Drew Point since the early-2000s as well as the complexities associated with unraveling the factors responsible for changing coastal permafrost bluffs in the Arctic.

Acknowledgements

BMJ, LMF, MX, and VER were supported by the National Science Foundation under grant OPP-1745369. G.G., I.N., and F.G. were supported by ERC 399 #338335, HGF ERC-0013, and ESA GlobPermafrost. Addition funding support provided by Sandia National Laboratory and the USGS. We would like to thank Paul Morin (Polar Geospatial Center at University of Minnesota) and Tom Cecere (U.S. Geological Survey) for tasking high-resolution satellite imagery for Drew Point. Any use of trade, product, or firm names is for descriptive purposes only and does not imply endorsement by the US Government.

References

AMAP 2017 Adaptation Actions for a Changing Arctic: Perspectives from the Bering-Chukchi-Beaufort Region. Arctic Monitoring and Assessment Programme (AMAP), Oslo, Norway. xiv + 255pp

Are´ F.E. 1988 Thermal abrasion of sea coast *Polar Geogr. and Geol.* 12 1-157.

Arp, C.D.; Jones, B.M.; Schmutz, J.A.; Urban, F.E.; Jorgenson, M.T. 2010 Two mechanisms of aquatic and terrestrial habitat change along an Alaskan Arctic coastline *Polar Biol.* 33(12) 1629-1640.

Atkinson, D.E. 2005 Observed storminess patterns and trends in the circum-Arctic coastal regime *Geo-Marine Lett.* 25(2-3) 98-109.

Ballinger, T.J.; Rogers, J.C. 2013 Atmosphere and Ocean Impacts on Recent Western Arctic Summer Sea Ice Melt *Geogr. Compass* 7(10) 686-700

Barnhart, K. R., Anderson, R. S., Overeem, I., Wobus, C., Clow, G. D., & Urban, F. E. 2014 Modeling erosion of ice-rich permafrost bluffs along the Alaskan Beaufort Sea coast Journal of Geophysical Research: Earth Surface 119(5) 1155-1179

417 Barnhart, K. R., Overeem, I., & Anderson, R. S. 2014 The effect of changing sea ice on the physical
418 vulnerability of Arctic coasts Cryosphere 8(5)
419 Barnhart, K. R., Miller, C. R., Overeem, I., & Kay, J. E. 2016 Mapping the future expansion of
420 Arctic open water Nature Climate Change 6(3) 280
421 Brown, J.; Jorgenson, M.T.; Smith, O.P.; Lee, W. Long- term rates of erosion and carbon input,
422 Elson Lagoon, Barrow, Alaska 2003 In *ICOP 2003 Permafrost: Proceedings of the 8th*
423 *International Conference on Permafrost* M. Phillips, S.M. Springman, and L.U. Arenson, (Eds.)
424 A.A. Balkema Publishers, Netherlands pp 101-106.
425 Couture, N.J., Irrgang, A., Pollard, W., Lantuit, H. and Fritz, M., 2018 Coastal erosion of
426 permafrost soils along the Yukon Coastal Plain and fluxes of organic carbon to the Canadian
427 Beaufort Sea Journal of Geophysical Research: Biogeosciences 123(2) 406-422
428 Dallimore, S.R.; Wolfe, S.A.; Solomon, S.M. Influence of ground ice and permafrost on coastal
429 evolution, Richards Island, Beaufort Sea coast, N.W.T. 1996*Can. J. of Earth Sci.* 33 664-675
430 Farquharson, L. M., D. H. Mann, D. K. Swanson, B. M. Jones, R. M. Buzard, and J. W. Jordan
431 2018 Temporal and spatial variability in coastline response to declining sea-ice in northwest
432 Alaska Marine Geology 404 71-83
433 Fritz, M., Vonk, J. E., & Lantuit, H. 2017 Collapsing Arctic coastlines. Nature Climate Change
434 7(1) 6
435 Gibbs, A.E., and Richmond, B.M. 2015 National assessment of shoreline change—Historical
436 shoreline change along the north coast of Alaska U.S.–Canadian border to Icy Cape: U.S.
437 Geological Survey Open-File Report 2015–1048 96 p
438 Gibbs, A.E., and Richmond, B.M. 2017 National assessment of shoreline change—Summary
439 statistics for updated vector shorelines and associated shoreline change data for the north coast of

Alaska, U.S.-Canadian border to Icy Cape: U.S. Geological Survey Open-File Report 2017–1107 21 p

Gibbs, A.E., B.M. Richmond, L.J. Erikson, and B.M. Jones 2018 Long-term retreat of coastal permafrost bluffs, Barter Island, Alaska. European Conference on Permafrost, Chamonix, 23 June to 01 July 2018

Gorokhovich, Y.; Leiserowiz, A. 2011 Historical and future coastal changes in northwest Alaska *J. of Coast. Res.* 28(1A) 174-186

Günther F, Overduin PP, Grosse G, Sandakov A, Grigoriev MN 2012 Thermo-erosion along the Yedoma coast of the Buor Khaya Peninsula, Laptev Sea, East Siberia. Proceedings of the 10th International Conference on Permafrost 137-142

Günther, F.; Overduin, P.P.; Sandakov, A.V.; Grosse, G.; Grigoriev, M.N. 2013 Short- and long-term thermo-erosion of ice-rich permafrost coasts in the Laptev Sea region *Biogeosciences* **2013** 10 4297-4318

Günther, F.; Overduin, P.P.; Baranskaya, A.; Opel, T.; Grigoriev, M.N. 2015 Observing Muostakh Island disappear: erosion of a ground-ice-rich coast in response to summer warming and sea ice reduction on the East Siberian shelf *The Cryosphere* 9 151-178

Hapke, C.J. 2005 Estimation of regional material yield from coastal landslides based on historical digital terrain modeling *Earth Surf. Process. Landf.* 30 679–697

Jones, B.M.; Hinkel, K.M.; Arp, C.D.; Eisner, W.R. 2008 Modern erosion rates and loss of coastal features and sites, Beaufort Sea coastline, Alaska *Arctic* 61 361-372

Jones, B.M.; Arp, C.D.; Jorgenson, M.T.; Hinkel, K.M.; Schmutz, J.A.; Flint, P.L. 2009a Increase in the rate and uniformity of coastline erosion in Arctic Alaska *Geophys. Res. Lett.* 36(3) *L03503*

462 Jones, B.M.; Arp, C.D.; Beck, R.A.; Grosse, G.; Webster, J.M.; Urban, F.E. 2009b Erosional
463 history of Cape Halkett and contemporary monitoring of bluff retreat, Beaufort Sea coast, Alaska
464 *Polar Geogr* 32(3-4) 129-142
465 Jorgenson, M.T.; Brown, J. Classification of the Alaskan Beaufort Sea Coast and estimation of
466 carbon and sediment inputs from coastal erosion. 2005 *Geo-Marine Letters 25*(2-3) 69-80
467 Kanevskiy, M. et al. 2012 Ground ice in the upper permafrost of the Beaufort Sea coast of Alaska.
468 *Cold Reg. Science and Technol 85* 56-70
469 Lantuit, H.; Overduin, P.P.; Couture, N.; Odegard, R.S. 2008a Sensitivity of coastal erosion to
470 ground ice contents: an Arctic-wide study based on the ACD classification of Arctic coasts. In
471 *NICOP 2008: Proceedings of the 9th International Conference on Permafrost*, D.L. Kane and
472 K.M. Hinkel (Eds.) pp. 1025-1029
473 Lantuit H.; Pollard W.H. 2008b Fifty years of coastal erosion and retrogressive thaw slump activity
474 on Herschel Island, southern Beaufort Sea, Yukon Territory, Canada *Geomorphology* **2008** 95 84-
475 102
476 Lantuit, H.; Atkinson, D.; Overduin, P.P.; Grigoriev, M.; Rachold, V.; Grosse, G.; Hubberten,
477 H.W. 2011 Coastal erosion dynamics on the permafrost-dominated Bykovsky Peninsula, north
478 Siberia, 1951-2006 *Polar Res* 30 7341
479 Lantuit H et al 2012 The Arctic Coastal Dynamics database: A new classification scheme and
480 statistics on Arctic permafrost coastlines *Estuaries and coasts* 35(2) 383-400
481 Lantuit, H.; Overduin, P.P.; Wetterich, S. 2013 Recent Progress Regarding Permafrost Coasts.
482 *Permafr. and Periglac. Process* **2013** 24(2) 120-130
483 Mars J. and Houseknecht, D. 2007 Quantitative remote sensing study indicates doubling of coastal
484 erosion rate in past 50 yr along a segment of the Arctic coast of Alaska *Geology* 35 583-586

485 Obu, J., Lantuit, H., Grosse, G., Günther, F., Sachs, T., Helm, V. and Fritz, M., 2017 Coastal
486 erosion and mass wasting along the Canadian Beaufort Sea based on annual airborne LiDAR
487 elevation data Geomorphology 293 331-346
488 J. Overland, E. Hanna, I. Hanssen-Bauer, S.-J. Kim, J. E. Walsh, M. Wang, U. S. Bhatt, and R. L.
489 Thoman, 2017 Surface air temperature [in "State of the Climate 2016"]. Bull. Amer. Meteor. Soc.,
490 98 (8) S93-S98
491 Overeem, I.; Anderson, R.S.; Wobus, C.W.; Clow, G.D.; Urban, F.E.; Matell, N. 2011 Sea ice loss
492 enhances wave action at the Arctic coast. *Geophys. Res. Lett. 38*(17) L17503
493 D. Perovich, W. Meier, M. Tschudi, S. Farrell, S. Gerland, S. Hendricks, T. Krumpen, and C. Haas
494 2017 Sea ice cover [in "State of the Climate 2016"]. Bull. Amer. Meteor. Soc 98 (8) S93-S98
495 Ping, C.L.; Michaelson, G.J.; Guo, L.; Jorgenson, M.T.; Kanevskiy, M.; Shur, Y.; Dou, F.; Liang,
496 J. 2011 Soil carbon and material fluxes across the eroding Alaska Beaufort Sea coastline. *J.*
497 *Geophys. Res* 116*, G02004*
498 Radosavljevic, B., Lantuit, H., Pollard, W., Overduin, P., Couture, N., Sachs, T., Helm, V. and
499 Fritz, M. 2016 Erosion and flooding—threats to coastal infrastructure in the Arctic: a case study
500 from Herschel Island, Yukon Territory, Canada Estuaries and Coasts 39(4) 900-915
501 Reynolds, R.W., N.A. Rayner, T.M. Smith, D.C. Stokes, and W. Wang, 2002 An improved in situ
502 and satellite SST analysis for climate J. Climate 15 1609-1625
503 Richter-Menge J (Ed) 2011 *Arctic report card 2010* DIANE Publishing
504 Romanovsky V E, Smith S L, Christiansen H H 2010 Permafrost thermal state in the polar
505 Northern Hemisphere during the international polar year 2007–2009: A synthesis *Permafr. and*
506 *Periglac. Process* 21 106-116

507 Schrader, F.C. A reconnaissance in northen Alaska across the Rocky Mountains, along the
508 Koyukuk, John, Anaktuvuk, and Colville rivers, and the Arctic coast to Cape Lisburne, in 1901,
509 with notes by W.T. Peters. *U.S. Geol. Surv. Prof. Paper* **1904**, 20, pp. 1-139.
510 Simmonds I and Rudeva I 2012 The great Arctic cyclone of August 2012 *Geophys. Res. Lett.*39
511 L23709
512 Smith SL et al 2010 Thermal state of permafrost in North America: A contribution to the
513 International Polar Year *Permafr. and Periglac. Process* 21 117-135
514 Steele, M., and S. Dickinson (2016), The phenology of Arctic Ocean surface warming, J. Geophys.
515 Res. Oceans, 121, 6847–6861, doi:10.1002/2016JC012089.
516 Thieler, E.; Himmelstoss, E.A.; Zichichi, J.L.; Ergul, A. 2009 The Digital Shoreline Analysis
517 System(DSAS) Version 4. 0- An ArcGIS Extension for Calculating Shoreline Change U. S.
518 Geological Survey 2009
519 Thomson, J., and W. E. Rogers 2014 Swell and sea in the emerging Arctic Ocean, Geophys. Res.
520 Lett. 41 3136–3140
521 Tweedie, C.E.; Aguire, A.; Vargas, C.S.; Brown, J. Spatial and temporal dynamics of erosion along
522 the Elson Lagoon Coastline near Barrow, Alaska (2002-2011) 2012 In *Proceedings of the Tenth*
523 *International Conference on Permafrost* 425-430
524 Tweedie, C. E.; Escarzaga, S. M.; Cody, R. P.; Manley, W. F.; Gaylord, A. G.; Aiken, Q.; Lopez,
525 A. F.; Aguirre, A.; George, C.; Nelson, L.; Brown, J. 2016 Patterns and Controls of Erosion along
526 the Elson Lagoon Coastline, Barrow, Alaska (2003-2016) American Geophysical Union, Fall
527 General Assembly 2016 abstract id. EP12B-02

528 Urban, Frank E., and Gary D. Clow 2016 DOI/GTN-P Climate and Active-layer Data Acquired in
529 the National Petroleum Reserve-Alaska and the Arctic National Wildlife Refuge, 1998-2014. US
530 Department of the Interior US Geological Survey 2016
531 Vermaire J C, Pisaric M F J, Thienpont J R, Courtney Mustaphi C J, Kokelj S V, Smol J P 2013
532 Arctic climate warming and sea ice declines lead to increased storm surge activity *Geophys. Res.*
533 *Lett.* 40 1386–1390
534 Walker, H.J. 1988 Permafrost and coastal processes *Proceedings of the Fifth International*
535 *Conference on Permafrost* **1988** 3 35-42
536 Walker H J 2005 Arctic coastal geomorphology *In* Encyclopedia of Coastal Science, Schwartz ML
537 (ed). Springer 49–55
538 Wendler, G.; Chen, L.; Moore, B. 2012 The First Decade of the New Century: A Cooling Trend
539 for Most of Alaska *Open Atmos. Sci. J.* **2012** 6 111-116
540 Wobus, C.; Anderson, R.; Overeem, I.; Matell, N.; Clow, G.; Urban, F. 2011 Thermal erosion of
541 a permafrost coastline: Improving process-based models using time-lapse photography *Arct.,*
542 *Antarct., and Alp. Res.* 43(3) 474-484
543

Tables

Table 1: Annual observations of coastal change and potential environmental forcing factors at Drew Point from 2007 to 2016. Mean, maximum, and daily OWD erosion values derived from high resolution satellite imagery. Storms and storm power value corresponding to the OWD between image acquisitions from the Drew Point Meteorological Station. Summertime thawing degree day (TDD) sums and near surface permafrost temperature (1.2 m depth) from June to November also derived from the Drew Point Meteorological Station. Sea surface temperatures (SST) derived from NOAA OISST V2 data from 71°N to 72°N and 155°W to 153°W.

Erosion Year	OWD (Days)	Mean Erosion (m)	Maximum Erosion (m)	Daily OWD Erosion (m)	Storms (Number)	Storm Power (m^2/s^2 day / storm number)	TDD (air)	PF Temp (° C - June to Nov)	SST (° C)
2007	84	22.2	41.7	0.26	9	1941	813	-3.37	3.5
2008*	107	15.9	48.8	0.15	9	1886	725	-3.06	2.3
2009*	96	19.4	44.1	0.20	13	2284	864	-3.05	2.7
2010	84	6.7	19.6	0.08	8	3027	874	-3.24	2.3
2011*	88	17.0	42.1	0.19	9	2115	850	-2.84	2.3
2012*	105	22.6	43.0	0.22	17	1857	1230	-2.94	2.0
2013*	98	13.4	31.7	0.14	15	1155	999	-2.89	1.5
2014*	71	16.5	32.7	0.23	11	4870	644	-2.61	2.0
2015	72	16.2	42.0	0.23	9	2484	947	-2.66	1.1
2016	107	22.0	47.6	0.21	14	1315	910	-2.57	2.0

*Indicates the time period between image acquistions spills over into adjacent open water season which has been accounted for.

Figures

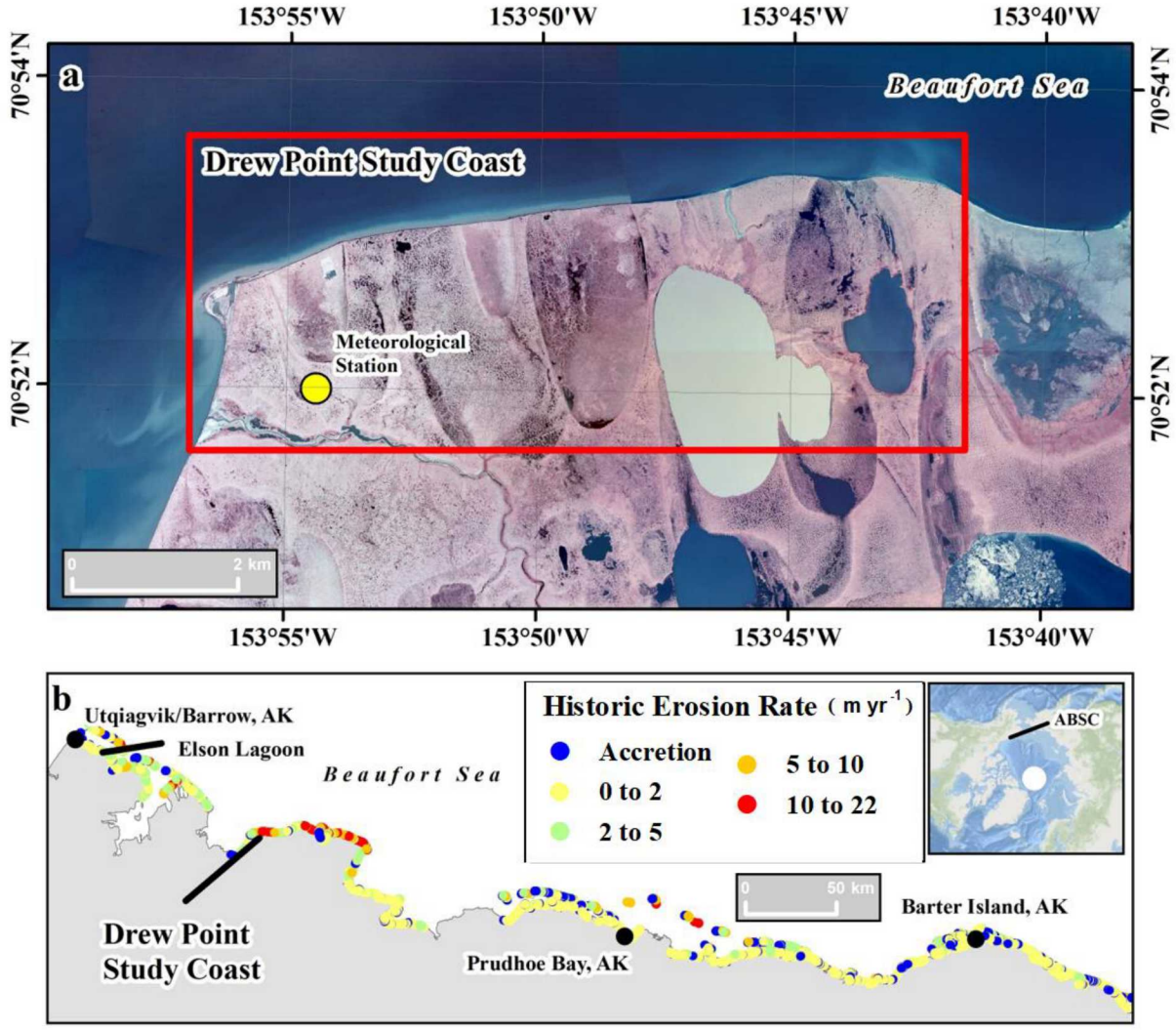

Figure 1. The Drew Point study area, Alaska Beaufort Sea Coast (ABSC). (a) The overlapping footprint of remotely sensed imagery used in this study is outlined with the red rectangle. The location of the meteorological station is shown with the yellow dot. (b) The location of Drew Point along the ABSC. Historic erosion rates from Gibbs and Richmond (2017) are shown for the period 1947 to 2010.

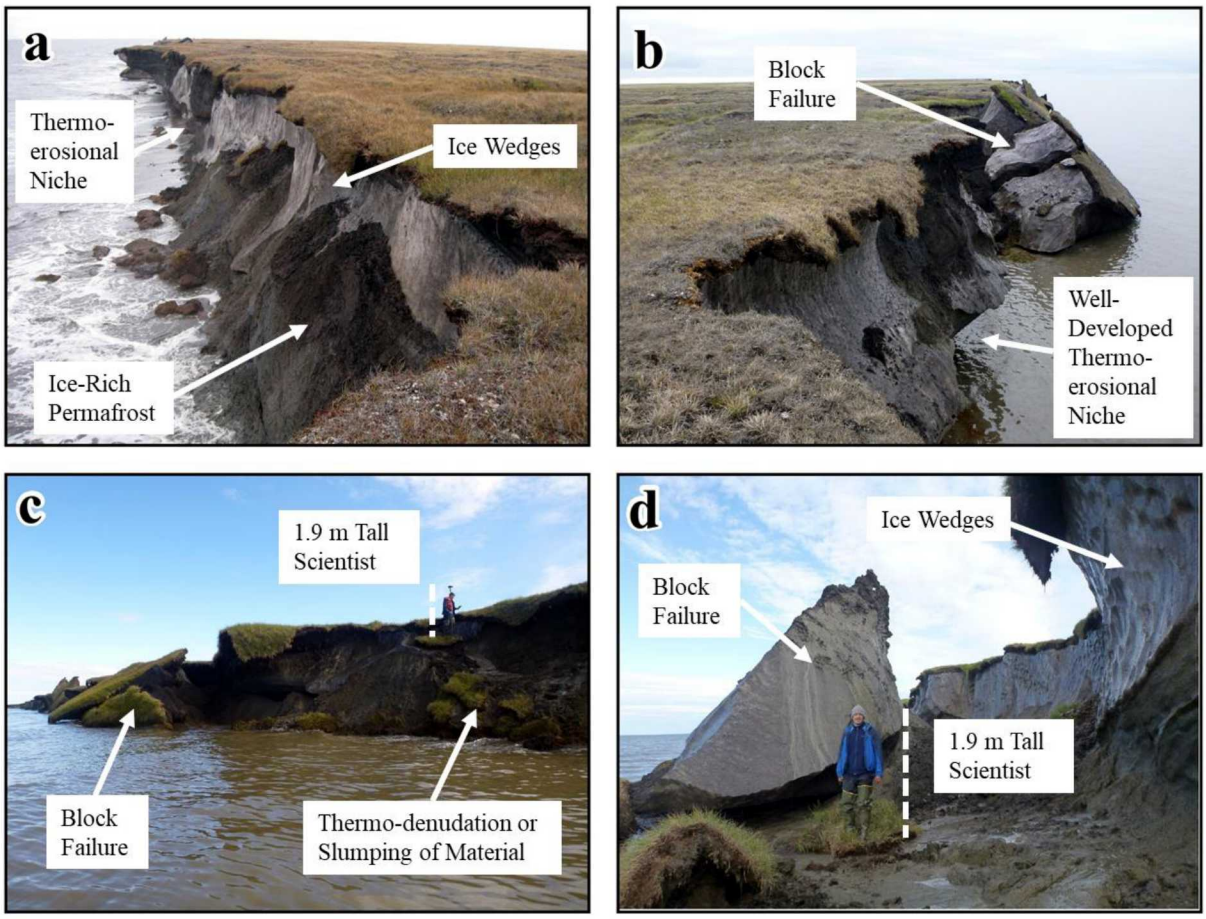

564
565
566 Figure 2. Field photographs demonstrating the dominant thermo-abrasion erosional process at
567 Drew Point. Photos from the study coast showing (a) the exposed ice-rich bluff face and
568 development of a niche prior to block collapse, (b) a well-developed niche and collapsed blocks
569 of permafrost, (c) looking back towards a 5 m high bluff from a small boat showing collapsed
570 blocks of permafrost as well as thermo-denudation to the right of the 1.9 m tall scientist, and (d)
571 the base of the bluff looking along a series of ice wedges (failure plane) showing the collapse of a
572 block of permafrost along a 7 m high bluff, with a 1.9 m tall scientist for scale.
573
574
575

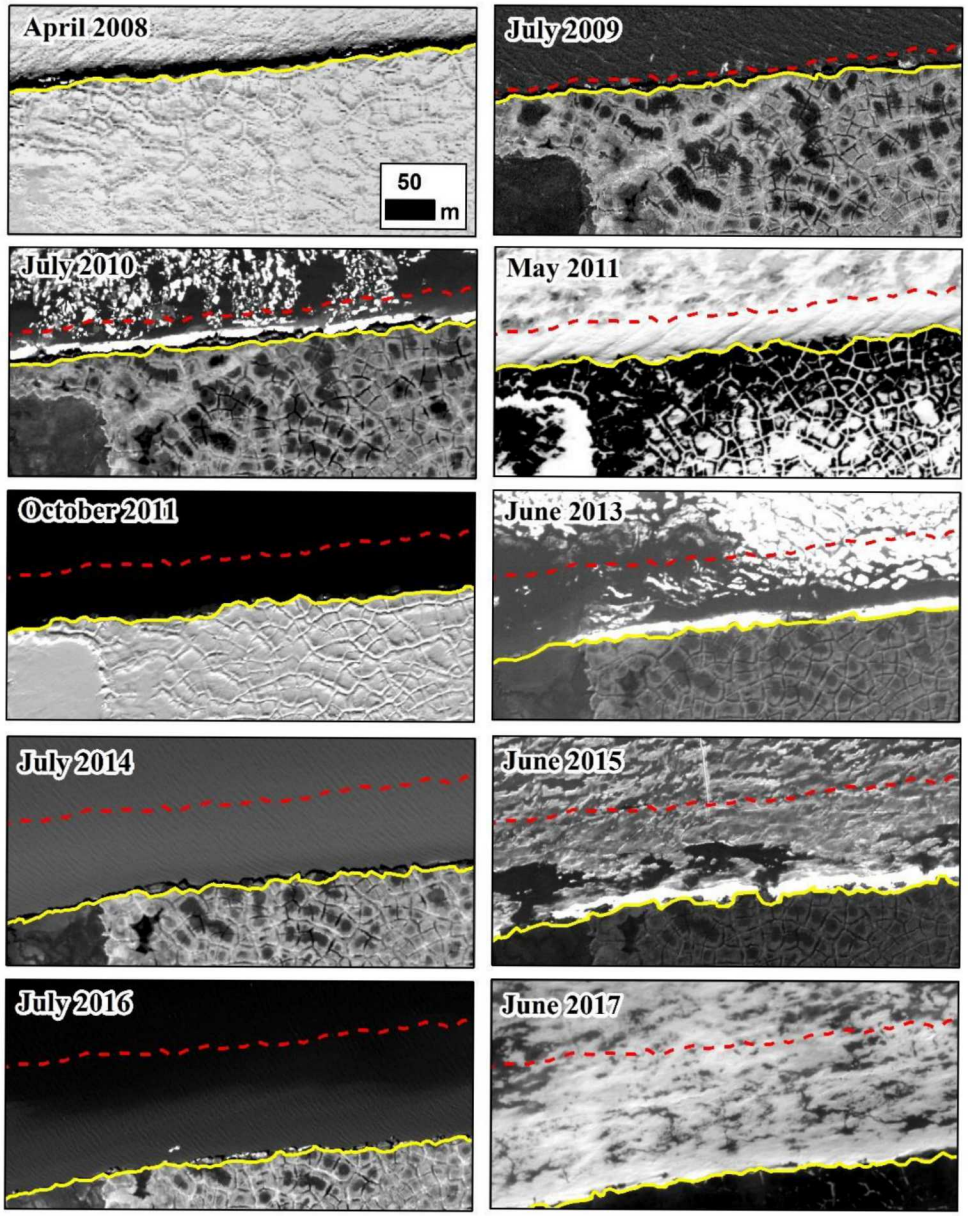

Figure 3: High resolution satellite images acquired for Drew Point between 2008 and 2017. The time series shows the same spatial domain in each frame at the same spatial scale. The respective coastal bluff position is shown in yellow in each frame. The red dashed line starting in July 2009 represents the 2008 coastline prior to the erosion season. More details on each image are provided in SOM Table 1. Images copyright of Digital Globe, Inc.

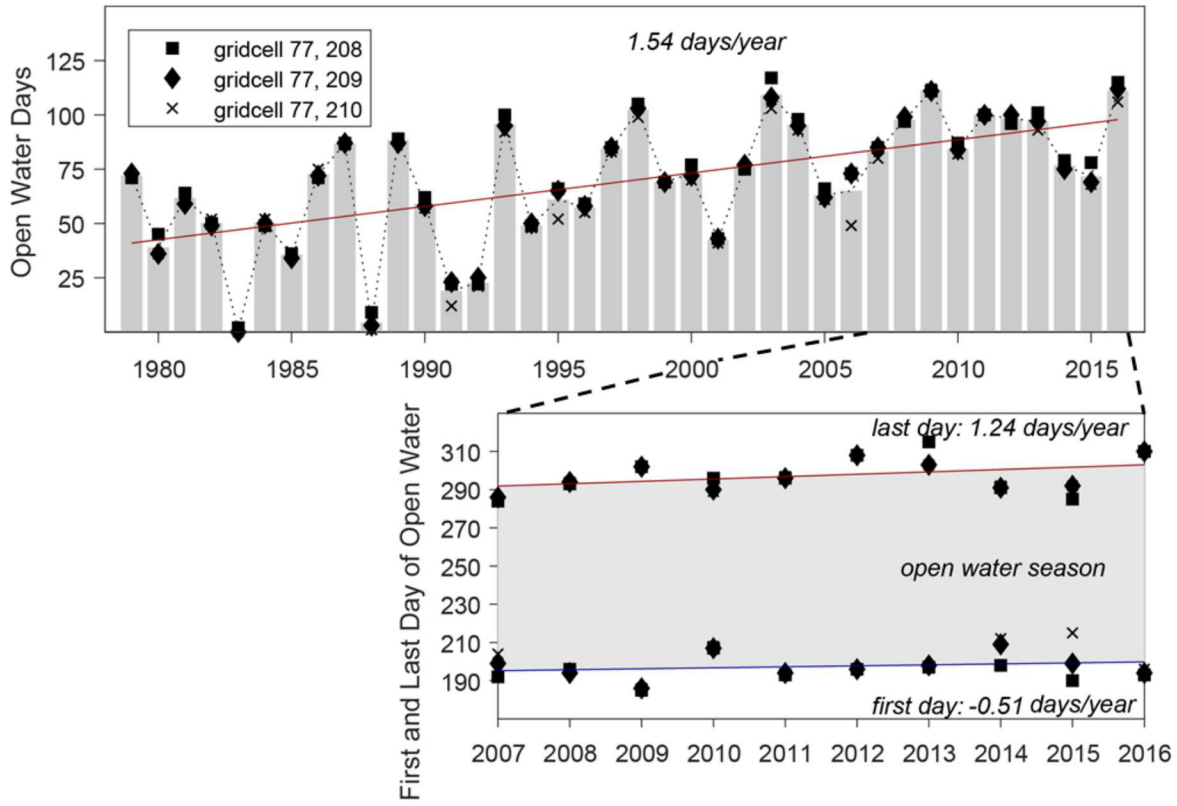

586

587 Figure 4. Open water duration determined at Drew Point from 1979 to 2016 using Nimbus-7
588 SMMR and DMSP SSM/I-SSMIS Passive Microwave Data from the National Snow and Ice Data
589 Center (NSIDC). (a) The number of open water days using three 25-km^2 nearshore pixels with
590 sea-ice concentrations < 15% to determine "open water" between 1979 and 2016. (b) The first
591 and last day of the open water season between 2007 and 2016 for the same three pixels near Drew
592 Point.

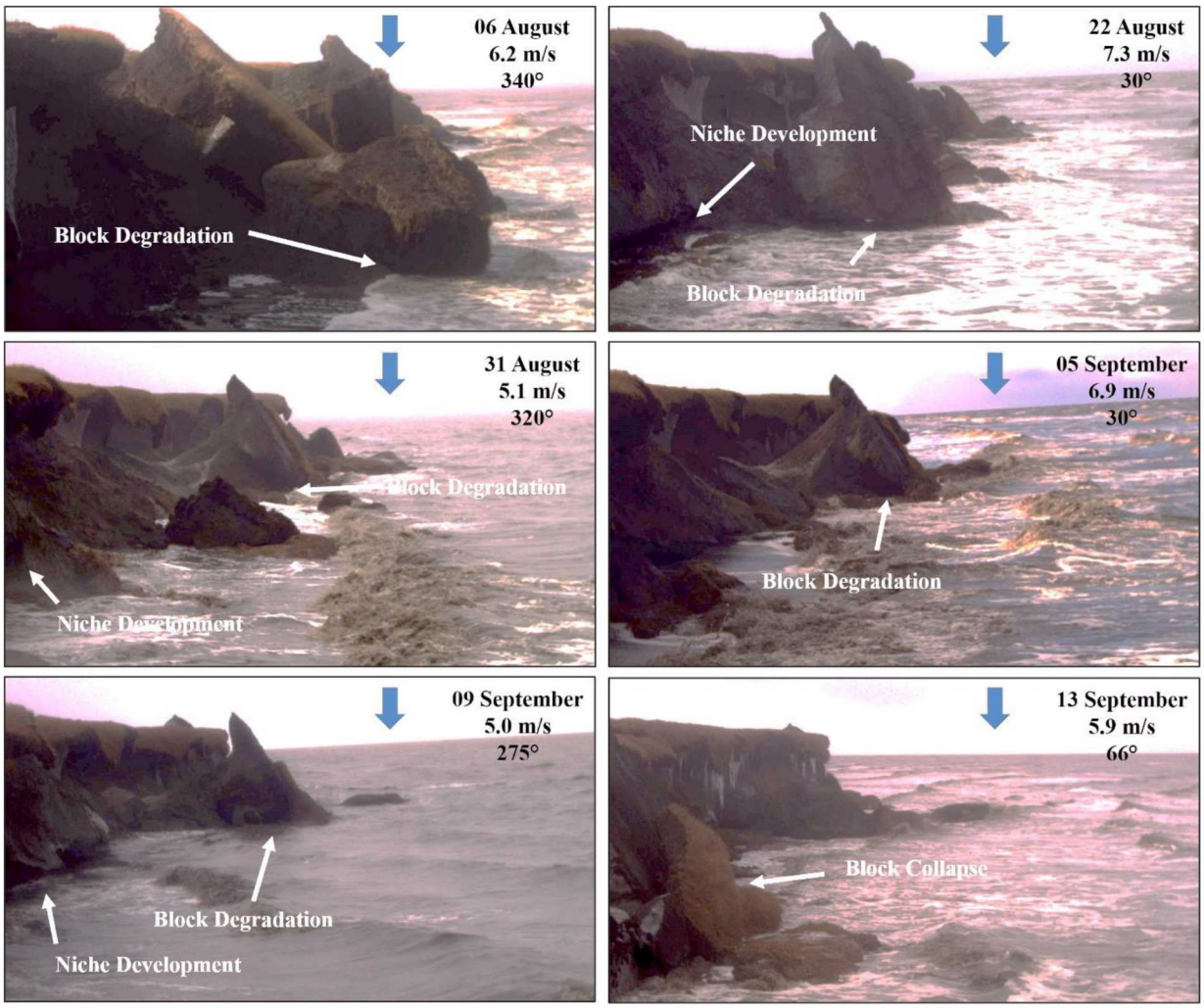

Figure 5: Time lapse camera observations between 06 August 2016 and 13 September 2016. The images show block collapse, block degradation, and niche development for westerly, northerly, and easterly wind events associated with winds speeds of at least 5 m/s. The blue arrow marks the starting bluff location in the 06 August image. Wind speed (m/s) and direction (°) are provided below each image date. More than 20 m of permafrost coastal bluff line erosion occurred at this site during the 2016 erosion season.

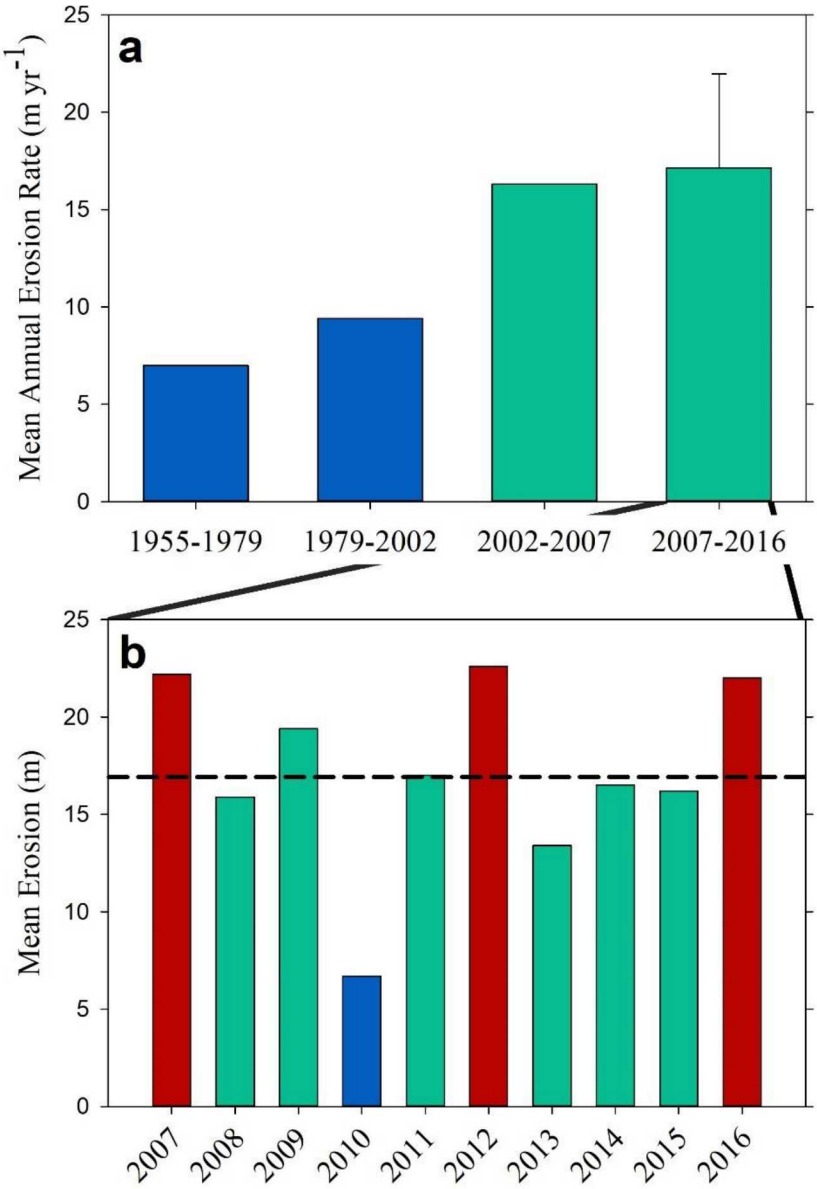

601

602 Figure 6: Permafrost coastal bluff erosion at Drew Point between 1955 and 2016. (a) Decadal-
603 scale mean annual erosion rates from 1955 to 1979, 1979 to 2002, and 2002 to 2007 (Jones et al.
604 2009a). Updated mean annual erosion rates for the past decade (2007 to 2016) presented in this
605 study. Error bar represents standard deviation in measured erosion during the last decade. (b)
606 Mean erosion from 2007 to 2016, based on annual erosion season determined by open water
607 duration, for the same 9-km segment of study coast as in (a). Erosion values between 5 to 10 m
608 shown in blue, 10 to 20 m shown in green, and greater than 20 m shown in red. The dashed line
609 in (b) represents the mean annual erosion between 2007 and 2016.

610

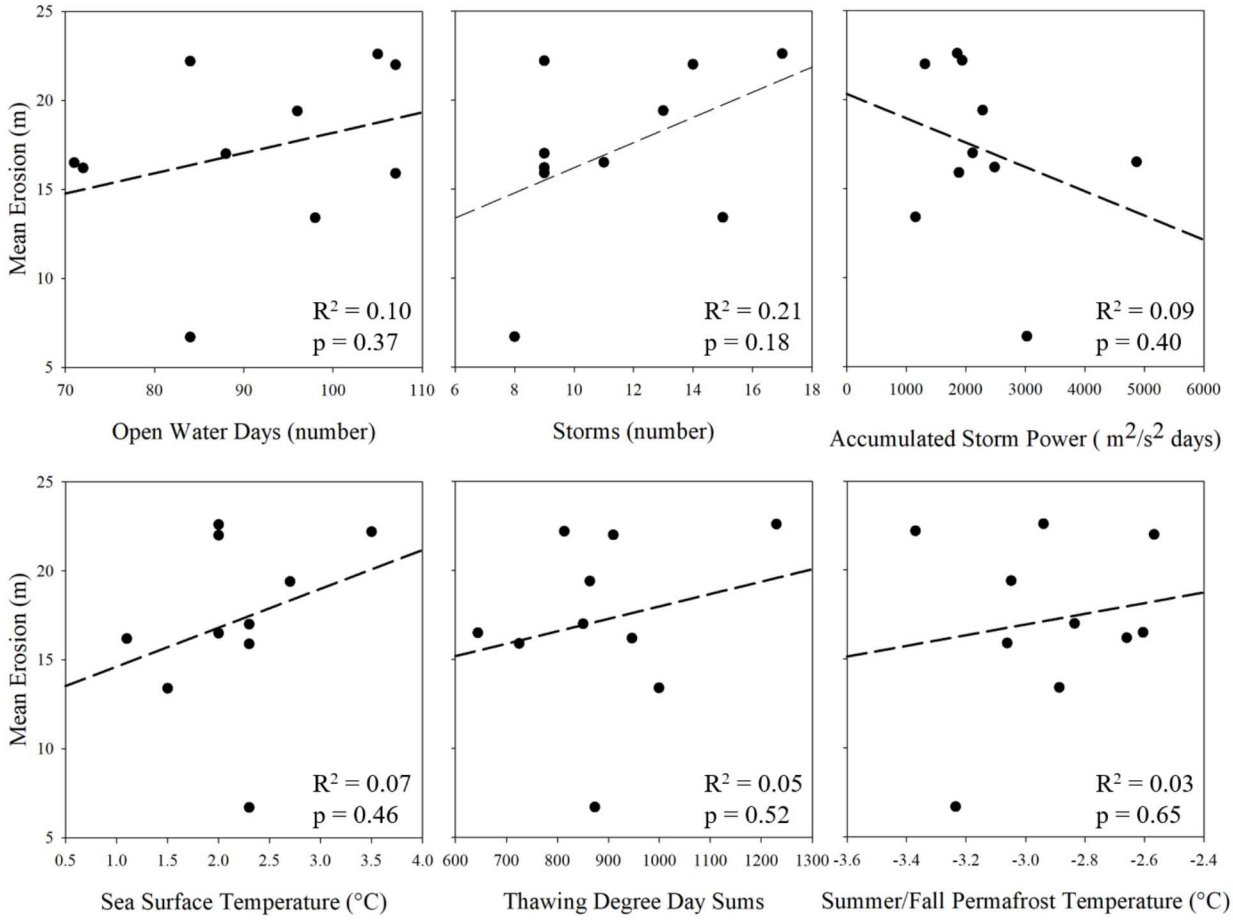

611

612 Figure 7: Scatterplots of mean erosion between 2007 and 2016 and potential environmental
613 forcing factors. Open water days derived from NSIDC, storms, storm power, thawing degree day
614 (TDD) sums, and near surface permafrost temperature (1.2 m depth) derived from the Drew Point
615 Meteorological Station, and sea surface temperature derived from NOAA OISST V2 data. All
616 plots show coefficient of determination and linear regression lines (dashed).

617

Supporting Online Material

Table 1: Erosion year, image type, image dates, spatial resolution, mean RMS georegistration error, manual digitization error, mean erosion, and dilution of accuracy for the high resolution time series analysis.

Erosion Year	Image Type	Image Date	Spatial Resolution (m)	Mean RMS Error (m)	Digitization Error (m)	Mean Erosion (m)	Dilution of Accuracy (m)
2007	Aerial Photo	19-Jul-07	2.5	2.4	0.14	22.2	3.6
	Quickbird	6-Apr-08	0.6	0.78	0.14		
2008	Quickbird	6-Apr-08	0.6	0.78	0.14	15.9	1.5
	Geoeye-1	20-Jul-09	1.0	0.61	0.14		
2009	Geoeye 1	20-Jul-09	1.0	0.61	0.14	19.4	1.4
	Worldview 1	9-Jul-10	0.5	0.63	0.14		
2010	Worldview 1	9-Jul-10	0.5	0.63	0.14	6.7	1.2
	Worldview 2	25-May-11	0.5	0.67	0.14		
2011	Worldview 2	25-May-11	0.5	0.67	0.14	17.0	1.3
	Worldview 1	9-Oct-11	0.5	0.85	0.14		
2012	Worldview 1	9-Oct-11	0.5	0.85	0.14	22.6	1.3
	Worldview 2	22-Jun-13	0.5	0.61	0.14		
2013	Worldview 2	22-Jun-13	0.5	0.61	0.14	13.4	1.3
	Worldview 2	30-Jul-14	0.5	0.87	0.14		
2014	Worldview 2	30-Jul-14	0.5	0.87	0.14	16.5	1.3
	Worldview 1	9-Jun-15	0.5	0.71	0.14		
2015	Worldview 1	9-Jun-15	0.5	0.71	0.14	16.2	1.3
	Worldview 2	7-Jul-16	0.6	0.73	0.14		
2016	Worldview 2	7-Jul-16	0.6	0.73	0.14	22.0	1.4
	Worldview 2	2-Jun-17	0.6	0.73	0.14		